Invited Paper

thermal blooming
Atmospheric optics
Lasers, high-energy
Beams

Twenty-Five Years of Thermal Blooming: An Overview

Frederick G. Gebhardt

Science Applications International Corporation
1040 Waltham Street, Lexington, MA 02173

ABSTRACT

Thermal blooming is one of the most important nonlinear effects on high energy laser beam propagation in the atmosphere. In this paper we give an overview of the progress made in the understanding of thermal blooming during the twenty-five years since the first observations were reported. Included is an historical overview and review of some of the key results and scaling parameters that are useful for understanding and describing steady-state whole-beam thermal blooming effects on high energy laser beam propagation both within the atmosphere and on a ground-to-space path through the atmosphere.

1. INTRODUCTION

When a high energy laser (HEL) beam propagates through the atmosphere, a small portion of the energy is absorbed by certain molecules and particulate matter in the air. The absorbed energy heats the air causing it to expand and form a distributed thermal lens along the atmospheric path that, in turn, spreads, bends and distorts the laser beam. This self-induced effect is called thermal blooming and, since it can limit the maximum power that can be efficiently transmitted through the atmosphere, is one of the most serious nonlinear problems encountered in the propagation of high energy laser radiation in the atmosphere. A wide variety of thermal blooming effects are relevant for high energy laser beams in the atmosphere. Many of these effects have been studied extensively and a number of detailed review articles have been written which describe most of the work prior to about 1980.[1-6]

Because of the recent intense interest in small-scale thermal blooming instabilities[7] it has become customary to refer to the large-scale thermal blooming effects which spread, bend and distort the entire beam as "whole-beam" thermal blooming. Since the small-scale blooming instabilities are addressed in the following paper as well as in a number of others in this volume, we will restrict our attention here primarily to the problem of whole-beam thermal blooming effects which represents the bulk of the work prior to 1985. It is interesting to note, however, that the initial interest in and studies of thermal blooming amplification of small-scale intensity perturbations or, stimulated thermal Rayleigh scattering (STRS), [8,9] occurred prior to most of the work on whole-beam blooming effects in the atmosphere.

In this paper we present an overview of the work that has been done on thermal blooming during the past twenty-five years. The emphasis here is to try to connect the extensive earlier results for whole-beam blooming effects with the more recent work on up-link thermal blooming compensation and related small-scale instabilities. Section 2 gives a brief historical overview outlining the particular types of blooming problems that have been studied during each of the major periods of work on blooming since the first observations of "thermal lens" effects in liquids were reported.[10,11] The fundamental thermal blooming equations for continuous wave (CW) and single-pulse (SP) laser beams are presented in Section 3. In Section 4 some of the basic results and scaling parameters for steady-state whole-beam thermal blooming effects in the atmosphere are reviewed. Here the blooming is characterized by isobaric heating with convection dominated heat transfer, due to the combined effects of wind and beam motion. The cases considered include both collimated and focused beams propagating within the absorbing atmosphere as well as that of a ground-based laser beam propagating through the atmosphere to a target in space. Conclusions are presented in Section 5.

2. HISTORICAL OVERVIEW

If one looks at the work on thermal blooming over the past twenty-five years one finds that it can be roughly divided into the following three periods based on the types and applications of the blooming problems being studied: (1) The Early Years/Infancy (1964-1969); (2) The Middle Years/Adolescence (1969-1979); and (3) The Late Years/Adulthood (1979-1989). The nature and emphasis of the thermal blooming work in these three periods is summarized as follows.

2.1 The Early Years/Infancy: 1964-1969

Work on whole-beam thermal blooming began with the first reported observation of a new "thermal lens effect" when transparent absorbing liquids (and some solids) were placed in a laser cavity.[10,11] The major emphasis initially was on the thermal blooming of stationary CW laser beams in liquids. With thermal conduction as the dominant heat transfer mechanism the dominant effect on the laser beam was the spreading produced by the negative lens-like refractive index gradient which naturally led to the use of terms like "thermal defocusing", "self-defocusing", "nonlinear defocusing", "self-induced divergence", etc.[12-16] Early interest in the thermal lens effect was in its practical application for low absorption measurements.[17-19] Another early application reported for the thermal lens effect was for its use as a power limiting device.[20] Interest in high energy laser beam propagation in the atmosphere led to the earliest studies of both small-scale[8,9] and whole-beam[21-24] convection dominated thermal blooming effects in gases.[15-18]

2.2 The Middle Years/Adolescence: 1969-1979

For the next five years or so extensive experimental and theoretical efforts were devoted to developing a basic understanding of atmospheric thermal blooming effects and their limits for CW, pulsed and repetitively pulsed (RP) high energy laser beam propagation.[1-5] The emphasis in these earlier studies was to develop a basic understanding of the physics of the thermal blooming process using simple and, more-or-less, idealized conditions to represent the characteristics of the laser beam and atmosphere. A number of detailed wave optics propagation codes were also developed to treat a wide variety of atmospheric thermal blooming problems.[1,2,4,5,25] Good agreement was obtained from comparisons of the results from the codes and laboratory simulation experiments.[4] Some of the special blooming problems studied, in addition to the important case of convection dominated blooming with wind and beam slewing, included the effects of beam jitter, optical turbulence, turbulent mixing, kinetic cooling, stagnation zones, non-coplanar wind and beam slewing, transonic slewing, aerosol blooming, and imaging through blooming. The use of focusing/defocusing, different beam profiles and aperture shapes and phase compensation were all considered as possible ways for correcting or reducing thermal blooming effects.[4] During the later years of this period the emphasis shifted toward: (a) the development of both detailed wave optics codes and systems level scaling laws for treating the combined effects of thermal blooming together with all relevant linear effects (e.g., nonideal beam quality, beam jitter, turbulence induced beam spreading and wander); and (b) the consideration of more realistic conditions for the laser beam, scenario and electro-optical and meteorological (EO-MET) properties of the atmosphere.

2.3 The Later Years/Adulthood: 1979-1989

During this most recent period the major emphasis has been on the problems of blooming and its compensation for ground-to-space HEL beam propagation. Interest also shifted from the longer infrared wavelengths of the 10.6 μm CO_2 and 3.8 μm DF lasers of greatest interest in the 1970's, to the much shorter near-UV, visible and near-infrared wavelengths to obtain the reduced diffraction losses/improved propagation efficiency required for the much longer ranges involved. The requirements for propagating large laser power densities at short wavelengths through the atmosphere for potential strategic missions resulted in significant renewed interest and research in the modeling of HEL beam propagation with adaptive phase correction of thermal blooming and turbulence. There has been an intense effort recently to understand and model the physics of both open- and closed-loop small-scale thermal blooming instabilities. The instabilities are strongly

seeded at short wavelengths by optical turbulence induced scintillation effects. Atmospheric velocity turbulence, on the other hand, is expected to be important in damping or reducing the small-scale growth. Small-scale blooming effects are of greater concern than whole-beam blooming for large phase compensated beams since their limits on the critical/largest correctable power are lower than those due to whole-beam effects.

3. BLOOMING BASICS

Thermal blooming refers to the general effects of self-induced phase distortion and the resulting distortion of the laser beam irradiance that occur when a laser beam propagates through an absorbing medium. The absorbed laser beam energy, which typically is only a very small fraction of the total laser beam energy, heats the medium causing localized gradients in the density and, hence, also the refractive index of the medium which, in effect, act as a distributed or thick nonlinear lens on the laser beam propagation. Since the laser beam heating of the absorbing medium usually results in the expansion and a decrease in refractive index of the medium in the region of the beam where the heating is greatest, the beam is usually defocused and spread, as suggested by the term "blooming". The exact nature of the thermal blooming effects on the laser beam generally depends, however, on a number of factors. These include: (1) the laser beam characteristics (i.e., wavelength, phase and irradiance distributions and the temporal mode, e.g., CW, single pulse (SP), or repetitively pulsed (RP)); (2) the kinetics of the absorption process, which determine the time required for the absorbed energy to heat (or, under certain special conditions with CO_2 laser beams, to cool[4]) the atmosphere; (3) the mode(s) of heat transfer that balance(s) the absorbed energy (e.g., thermal conduction, natural or free convection, forced convection or the generation of sound waves); (4) the time scale of interest (e.g., transient versus steady-state conditions); and, (5) the propagation medium and scenario characteristics (e.g., the pathlength, optical properties, platform speed, slewing, etc.).

3.1 Governing Equations

The basic governing equations for the thermal blooming effects on the laser beam complex field u (R) are (1) the time-independent paraxial scalar wave equation

$$\left[2ikn(R)\left(\frac{\partial}{\partial z} + \frac{\kappa_e}{2}\right) + \nabla^2 + k^2 n^2(R)\right] u(R) = 0 \qquad (1)$$

and, (2) the equation for the refractive index of the absorbing medium

$$n(R) = n_o + n_B\,(\alpha I(R)). \qquad (2)$$

The envelope of the wave function u is assumed to change slowly compared with the propagation time and the phase gradients are assumed to be small due to the heating effects. We have suppressed the harmonic time factor exp (-iωt) for the function u, $k = \omega/c = 2\pi/\lambda$ is the free-space propagation constant with c and λ the speed of light and wavelength in vacuum, and $\kappa_e = \alpha + \sigma$ is the extinction coefficient of the medium with α and σ being the absorption and scattering coefficients, respectively. The refractive index n consists of a constant background value n_o and the blooming contribution n_B which is a function of the absorbed laser beam power density $\alpha I = \alpha |uu^*|$.

3.2 Isobaric Heating

For CW laser beams (and, also RP beams with negligible SP blooming) in the atmosphere it is customary to assume that the heating occurs instantaneously and that the heating rate is sufficiently small that pressure disturbances are negligible. Thus, with the heating assumed to be isobaric, i.e., at constant pressure,

the blooming contribution to the refractive index is given by $n_B = n_T T_B$ where $n_T = dn/dT = -(n_o - T_o)/T_o$ is the refractive index change with respect to temperature of the gas at constant pressure and T_B, the temperature rise due to laser heating, is given by the energy balance equation

$$\rho C_p \left[\frac{\partial}{\partial t} + \vec{v}.\nabla - \frac{K}{\rho C_p}\nabla^2\right] T_B = \alpha I \qquad (3)$$

Equations (1) - (3) are used to describe the transient development and steady-state solutions for the thermal blooming of a CW or RP laser beam when both thermal conduction and convection heat transfer are present.

Thermal conduction dominated blooming, described by the third term in (3), occurs when the beam is stationary (i.e., v = 0) and for early enough times or small enough heating that natural convection is still negligible. The basic requirement is that the natural convection velocity v must be much less than χ/a, where $\chi = K/\rho C_p$ is the thermal diffusivity of the medium, with K, ρ and C_p, respectively, the thermal conductivity, density and specific heat at constant pressure, and a is either the beam radius (for the case of whole-beam blooming) or the smallest scale size of interest in the case where small-scale blooming effects on very large uniform intensity beams are of concern. Estimates for the natural convection velocities for liquids and gases with a horizontal beam are given by Smith.[4]

A dimensionless scaling parameter for the magnitude of the steady-state conduction dominated blooming effect on the laser beam intensity is given by[4]

$$D_C = -\frac{n_T \alpha P z^2}{2\pi n_o K a^2} \qquad (4)$$

The on-axis intensity decrease in the beam due to blooming after propagating a distance z through the absorbing medium is given approximately by $\exp(-D_C)$. This expression is based on a perturbation solution and applies for a Gaussian beam with 1/e intensity radius a when $\alpha z << 1$ and diffraction effects are negligible, i.e., the Fresnel number $N_F = ka^2/z >> 1$. Conduction dominated blooming using Eq. (4) has also been used as a convenient and direct method for measuring the eddy diffusion coefficient K_h for a turbulent medium in a study of velocity turbulence effects on blooming.[26] Early studies of conduction dominated blooming are described in References 10-20 and 23.

The heat transfer and associated thermal blooming is convection dominated according to (3) when the velocity $v >> \chi/a$. This condition is virtually always met for laser beam propagation in the atmosphere since $\chi \approx 0.2$ cm^2/s for air and χ/a for any beam or scale sizes a of practical interest is negligible compared with almost any except absolutely calm wind conditions. Because of the importance of the convection dominated blooming problem for atmospheric propagation it has been studied the most extensively. The dominant features of this type of blooming are for an initially symmetrical circular beam to form a non-symmetrical crescent shaped pattern which is spread or bloomed symmetrically transverse to the wind direction and with the peak intensity along the wind direction being shifted into the wind. Some of the key scaling parameters and models and laboratory simulation experiment and wave optics propagation code results for convection dominated whole-beam blooming effects in the atmosphere will be reviewed in Section 4.

3.3 Non-Isobaric Heating

For very short high intensity laser beam pulses the isobaric heating assumption does not apply since the heating results in significant pressure and density disturbances which propagate across the beam at the acoustic velocity C_s. To determine the transient blooming contribution to the refractive index for intense short laser pulses the density change ρ_B due to the non-isobaric laser beam heating must be found. Combining the

hydrodynamic equations of mass, momentum and energy conservation gives the following equation for the transient or single pulse density change ρ_B.[4]

$$\left(\frac{\partial^2}{\partial t^2} - C_s^2\nabla^2\right) \frac{\partial \rho_B}{\partial t} = (\gamma - 1)\alpha\nabla^2 I \qquad (5)$$

Here $\gamma = C_p/C_v$ is the ratio of specific heats for the medium. With ρ_B given by (5) and the refractive index by $n_B = -n_T (T_o/\rho_o)\, \rho_B$, where T_o and ρ_o are the ambient temperature and density, Eqs. (1) and (2) are used to calculate the transient or single pulse thermal blooming effects.[4] Simple scaling parameters have been found for the two limits of (1) the pulse length t_p being either very short or (2) very long compared with the acoustic transit time $t_a = a/C_s$ across the beam. For the short time regime $t_p << t_a$, the density disturbance grows as t^3. The thermal blooming in this case is called t-cubed blooming and, for a fixed absorbed energy, can be made negligible by reducing the pulse length. In the long pulse regime where $t_p >> t_a$, the density disturbance is proportional to the absorbed energy which grows linearly with time. Clearly, to avoid or minimize single pulse blooming effects the pulse length should always be very short compared to the acoustic transit time.[2-4,6]

With the propagation of repetitively pulsed beams we must consider both the single-pulse blooming effects just mentioned as well as the steady-state isobaric blooming that results from the overlap of density disturbances in the beam path due to the heat deposited into the air by previous pulses. Steady-state repetetively pulsed blooming effects can be avoided if the pulse repetition frequency (PRF) is low enough to allow the heated air from previous pulses to be cleared from the beam path by the wind or beam motion. As the PRF increases the pulse overlap blooming effects increase until, in the limit of many pulses-per-flow-time (PPFT) of the air across the beam (e.g., PPFT > 10-20 for a beam without slewing), the blooming approaches that for the steady-state CW beam case. Propagation limits due to blooming for CW and RP beams are compared in Reference 3.

4. STEADY-STATE BLOOMING WITH WIND/BEAM MOTION

In this section we review the important problem of steady-state whole-beam blooming effects with wind or beam motion. We consider first the simplest case of a collimated beam in a homogeneous absorbing and moving medium. Next the more general case of a focused beam in a medium with inhomogeneous heating and relative motion of the beam and medium is considered. The thermal blooming for ground-to-space propagation is addressed in the last section.

4.1 Collimated Beam-Homogeneous Path

Figure 1 shows a qualitative sketch of a CW laser beam propagating in an absorbing medium, such as a horizontal path in the atmosphere, where the absorption α and cross-wind speed v are uniform. As the air moves across the beam the temperature increases due to the absorbed energy from the laser beam. This causes the density of the air and, also the refractive index, which is proportional to the density, to decrease as the air moves across the beam. The temperature and refractive index variations across the beam center along the wind direction are shown in Figure 1. Since light rays bend in the direction of increasing refractive index, the central ray is shown in the sketch to be bending into the wind. The net result is that the irradiance profile becomes distorted with its peak shifted into the wind.

A convenient and useful measure of the strength and overall characteristics of the thermal blooming effect is given by the optical phase distortion produced by a small section of the thermal lens. The steady-state phase shift due to blooming for the path length z, which we assume to be short enough that the beam irradiance distribution is undisturbed by the blooming and the attenuation due to absorption and scattering are negligible (i.e., the extinction number $N_E = \kappa_e z << 1$), is given by

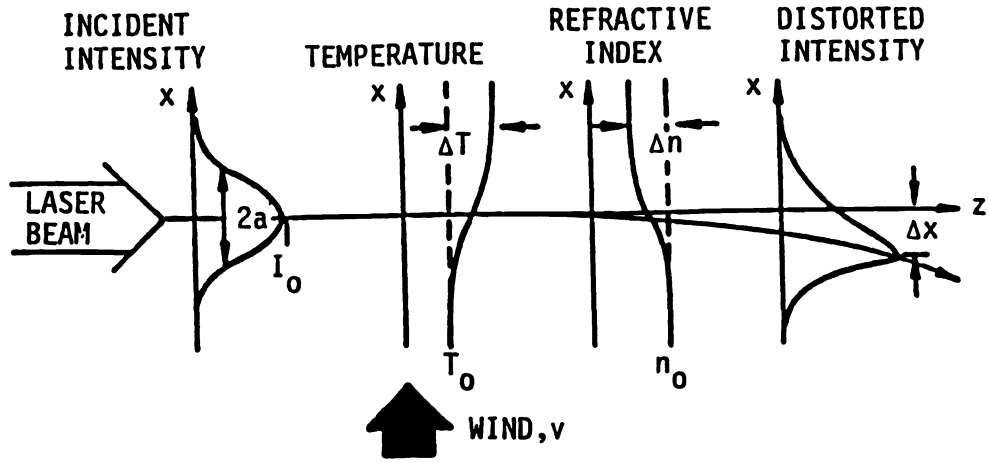

Figure 1. Sketch of the steady-state thermal blooming problem with wind.

$$\varphi_B(x,y) = kn_T\left(\frac{\alpha z}{\rho C_p v}\right)\int_{-\infty}^{x} I(x',y)\,dx' \tag{6}$$

Here we have assumed isobaric heating where the refractive index distortion due to blooming is $n_B = n_T T_B$ and that T_B is given by Eq. (3) in the steady-state limit for the convection dominated case. Assuming in Eq. (6) the irradiance distribution for a Gaussian beam, $I = (P/\pi a^2)\exp(-r^2/a^2)$, with P the laser beam power and $D = 2\sqrt{2}a$ the $1/e^2$ intensity beam diameter, the blooming phase is

$$\varphi_{BG}(x,y,z) = -\frac{\Delta\varphi_G}{2}\exp[-(y/a)^2]\,[1 + \mathrm{erf}(x/a)]$$

$$\simeq -\frac{\Delta\varphi_G}{2}\left\{1 + \frac{2}{\sqrt{\pi}}\left(\frac{x}{a}\right) - \left(\frac{y}{a}\right)^2 - \frac{2}{\sqrt{\pi}}\left[\frac{1}{3}\left(\frac{x}{a}\right)^3 + \left(\frac{x}{a}\right)\left(\frac{y}{a}\right)^2\right] + \frac{1}{2}\left(\frac{y}{a}\right)^4 \cdots\right\} \tag{7}$$

The maximum phase shift in radians across the beam along the wind direction is

$$\Delta\varphi_G = (1/2\sqrt{\pi})\,N_D \tag{8}$$

where

$$N_D = \frac{4\sqrt{2}(-n_T)k\alpha Pz}{\rho C_p v D} \tag{9}$$

is the Bradley-Hermann[27] distortion number commonly used as a measure for the strength of the thermal blooming. The number of waves N_λ of blooming phase across the beam is now also often used as a measure of the amount of blooming and, from (8) we have that $N_\lambda = \Delta\varphi_G/2\pi = (1/4\pi^{3/2})\, N_D$.

Referring to the series expansion of the blooming phase in (7) we see the leading linear term in x and the quadratic term in y which produce, respectively, the prism or beam bending effect along the wind direction and the negative lens or defocusing effect perpendicular to the wind. These dominant blooming effects on the beam are shown in Figure 2 along with the phase distributions along and perpendicular to the wind direction.

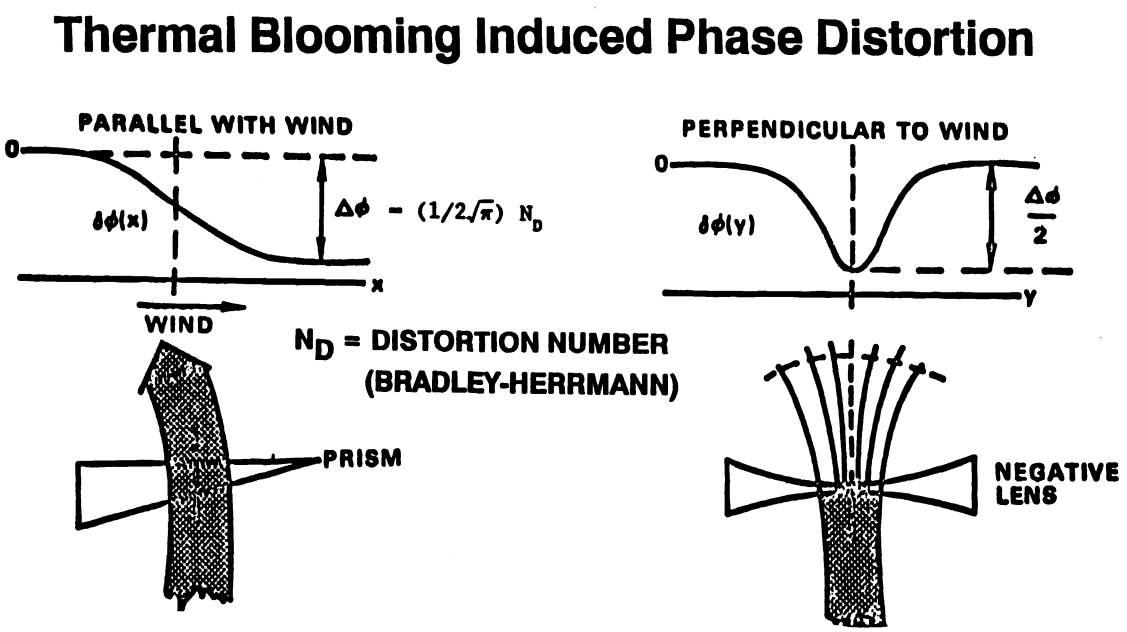

Figure 2. Dominant blooming effects in a wind.

The leading terms in the series expansion Eq. (7) of the blooming phase can also be identified with the primary or Seidel aberrations of classical aberration theory.[28] In particular, the linear term which bends the beam is referred to as distortion and, in this case, is of the pincushion type.[29] The quadratic term in y responsible for beam spreading is called astigmatism. The third-order term is coma and the fourth-order term corresponds to spherical aberration for a cylindrical element.

The blooming phase for a uniform irradiance circular beam is also frequently of interest and, using (6), is given by

$$\varphi_{BU}(x,y,z) = -\,(\Delta\varphi_U/2)\,\left[\,(x/R_M) + (1 - y^2/R_M^{\,2})^{1/2}\right]$$

$$\simeq -\,(\Delta\varphi_U/2)\,\left[\,1 + (x/R_M) - (y^2/2R_M^{\,2}) - (y^4/8R_M^{\,4}) \ldots\right] \qquad (10)$$

where R_M is the beam radius (D/2) and the total phase shift across the beam is

$$\Delta\varphi_U = (1/\sqrt{2}\pi)\, N_D \qquad (11)$$

It is interesting to note that there is no third-order coma term in the blooming phase for the uniform beam. The beam distortion in this case tends to be more elliptical rather than crescent shaped as for the Gaussian beam.

Some of the important characteristics of the blooming phase are compared in Table 1 for the uniform, infinite Gaussian and truncated Gaussian beam shapes. These include: (1) The total blooming phase $\Delta\varphi$, in radians across the beam; (2) The effective tilt angle, θ_t, in radians for the beam bending into the wind; (3) The negative lens focal length, f_B, for the beam defocusing transverse to the wind; and, (4) The maximum phase gradient, MAX φ', which occurs near the hotter, down-wind edge of the beam. Comparison of the tilt angles and negative lens focal lengths for the different beam shapes readily shows these blooming effects to be much smaller for the uniform beam than for the two Gaussian beam shapes.

Table 1. Blooming Phase Characteristics for Several Beam Shapes.

		Uniform	Infinite Gaussian	Truncated Gaussian
Total:	$\Delta\varphi/N_D$	0.225	0.28	0.31
Tilt:	$\theta_t/(N_D\lambda/D)$	1/28	1/13.8	1/12.6
Focal Length	$f_B/(kD^2/N_D)$	2.22	0.44	0.40
Gradient:	MAX φ' $/(N_D/D)$	0.69*	0.65	0.75

*Uniform beam gradient at x/D = 0.43, y/D = 0.475.

To determine the change in the laser beam irradiance pattern as a result of thermal blooming requires the solution of the scalar wave equation (1) with the irradiance dependent refractive index expression n_B as given in (6). Although a number of detailed wave-optics propagation codes have been developed to accurately solve this complex nonlinear propagation problem, much useful insight, including a nondimensional scaling parameter for the thermal blooming induced irradiance changes, can be obtained from a perturbation solution of (1) with diffraction effects neglected.[30]

The general perturbation solution, valid in the ray-optics limit, for the laser beam irradiance after propagation through a medium with arbitrary refractive inhomogeneities n(R) is[30]

$$I(x,y,z) = I_0(x,y,z)\ \exp\left\{ -\int_0^z \left[\nabla + \frac{\nabla I}{I}\right] \cdot \int_0^{z'} \frac{\nabla n}{n_0}\, dz''\, dz' \right\} \qquad (12)$$

where I_o is the unperturbed irradiance. Assuming the unperturbed Gaussian irradiance $I_o = (P/\pi a^2)$ $\exp[-(x^2 + y^2)/a^2]$ and weak absorption ($\alpha z << 1$), for which the blooming index n_B is given by φ_{BG}/k in Eq. (7), using Eq. (12) for the thermally bloomed irradiance pattern yields[30]

$$\frac{I(x,y,z)}{I_0} = \exp\left\{- N_C \left[2\left(\frac{x}{a}\right) e^{[-(x^2+y^2)/a^2]} + \frac{\sqrt{\pi}}{2} e^{[-y^2/a^2]} (1 - 4y^2/a^2)[1 + \text{erf}(x/a)]\right]\right\} \quad (13)$$

Here, N_C is the collimated beam irradiance distortion parameter for blooming with a wind, given by

$$N_C = \frac{16\sqrt{2}(-n_T)\alpha P z^2}{\pi n_0 \rho C_p V D^3} \quad (14)$$

The beam distortion parameter N_C can also be written as

$$N_C = (1/2\pi)\ N_D/N_F \quad (15)$$

where $N_F = kn_0D^2/8z$ is the Fresnel number. According to (15) the magnitude of the blooming phase distortion, i.e., N_D, must increase with the Fresnel number N_F, to obtain the same amount of beam distortion, as measured by N_C. For small values of N_C the peak intensity, normalized by the undistorted value, decreases as $1 - (\sqrt{\pi}/2)N_C$ and its position is shifted into the wind direction by the amount $\Delta x/a \approx (3/2)N_C$.

The distorted beam irradiance patterns in Figure 3, which apply in the ray-optics limit ($N_F >> 1$), have been calculated numerically by iterative application of the above perturbation solution.[30]

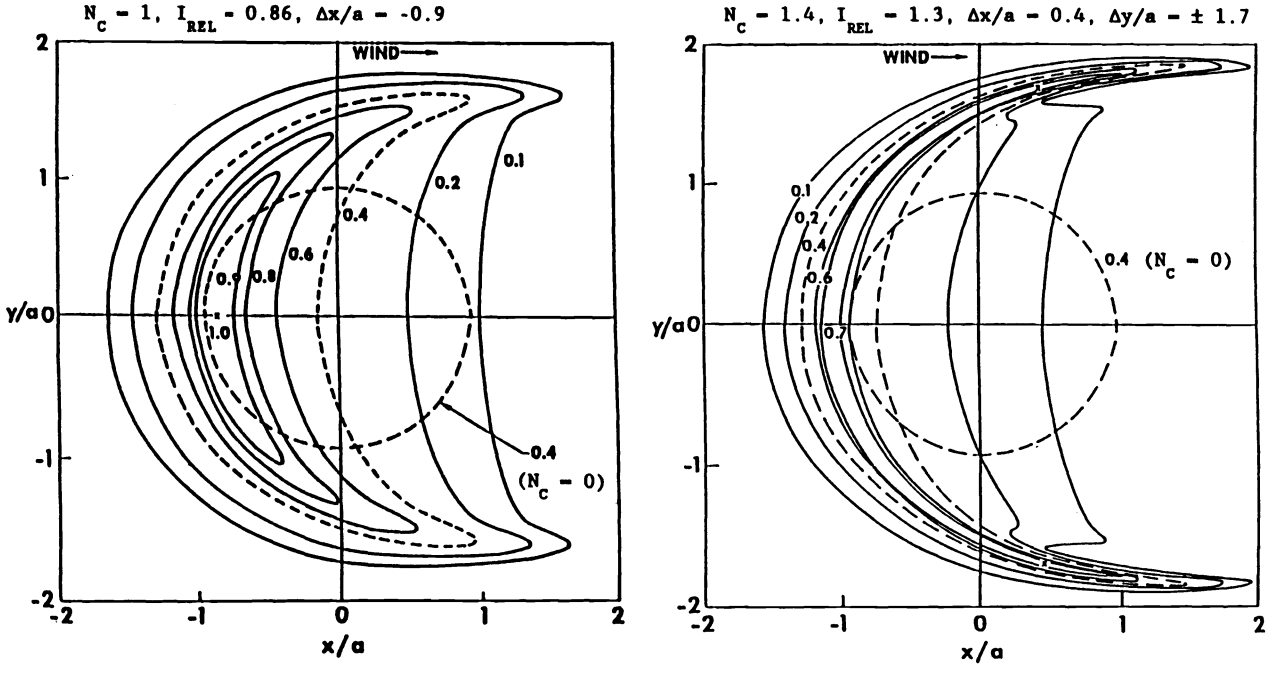

Figure 3. Calculated bloomed irradiance contours for N_C = 1 and 1.4, in the ray-optics limit[30]

The bloomed intensity patterns show the characteristic crescent shape with beam spreading transverse to the wind, the peak intensity shifted into the wind and, also, a significant focusing effect along the wind direction. For the N_C = 1 case the peak intensity is about 0.86 times the undistorted value and the peak has shifted almost one beam radius into the wind. For the N_C = 1.4 case, however, the peak intensity point has shifted from the beam axis along the flow to the wings of the crescent and the thermal focusing has increased it to ~ 1.3 times the unperturbed value. The intensification effect due to the blooming with wind/beam motion was first observed in liquid cell experiments,[31] which were conducted with an argon-ion laser at λ = 0.5145 μm. In the first experiments[22,32] to observe and study the blooming effects due to a wind, which were done in gas (i.e., a small recirculating wind tunnel) with a 10.6 μm CO_2 laser beam, the intensification effect was not observed. The bloomed intensity was found to only decrease, even for very large distortion conditions.

Subsequent computer calculations, with diffraction effects included, and further experiments at 10.6 μm with moving liquid cells, confirmed what had been suspected earlier, i.e., the reason the intensification wasn't observed in the earlier gas experiments was due to the much stronger influence of diffraction which tended to counteract or limit the thermal self-focusing tendency at the small Fresnel numbers (~2.5) of those experiments.[33] Figure 4 shows calculated and experimental results for the effects of diffraction on the relative intensity change with blooming, as functions of the beam distortion number N_C and the Fresnel number N_F.[33] Based on these results, intensification with blooming requires a Fresnel number of ~20 or more. It is interesting to note that the shift of the peak intensity into the wind does not show any significant dependence on the Fresnel number.

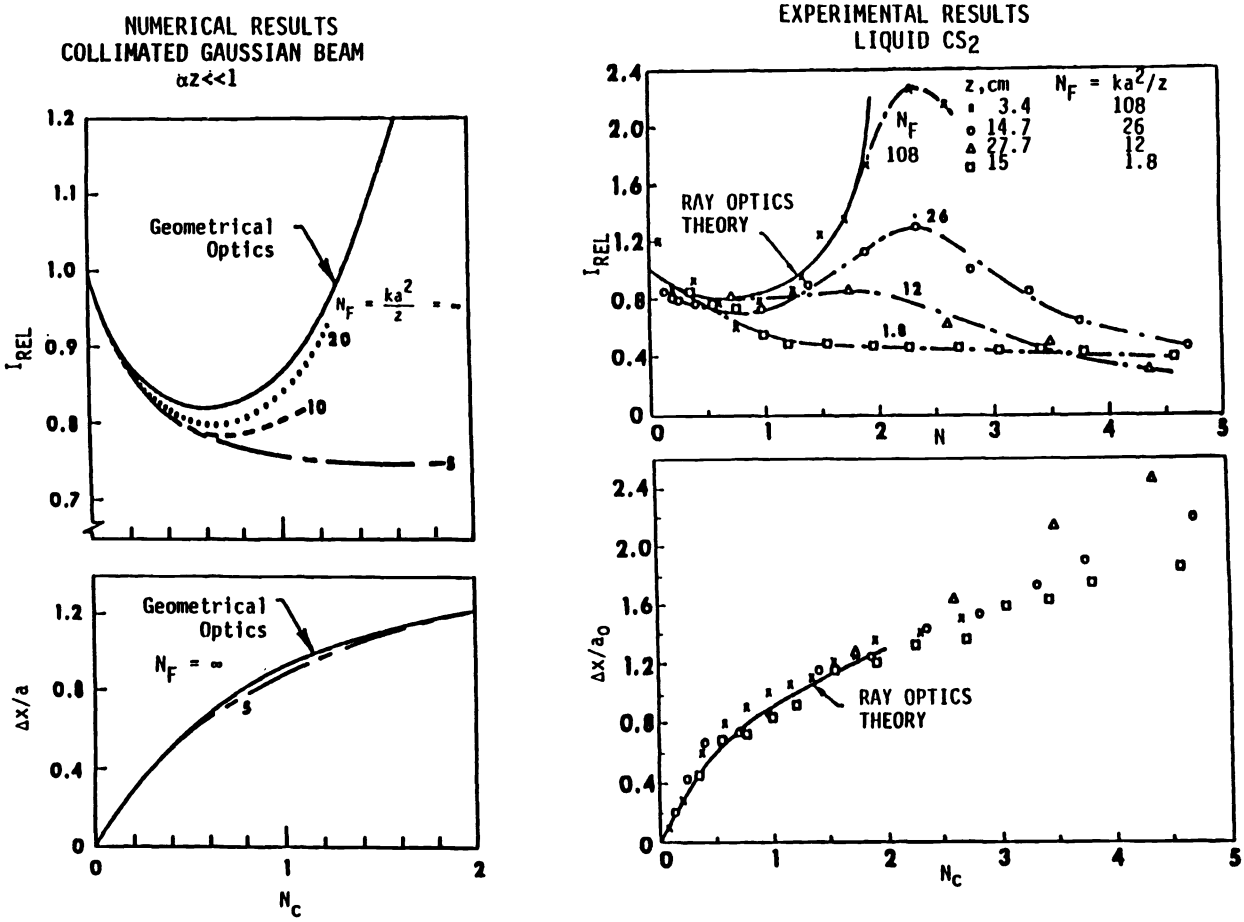

Figure 4. Peak intensity and deflection for collimated beam blooming[33]

Figure 5 compares the distorted and undistorted beam profiles at the same beam distortion number of $N_C \approx 2$ for the Fresnel numbers of 108, 26, 12 and 1.8. From the results in Figures 4 and 5 it is clear that diffraction effects strongly compete with and limit the self-focusing tendency of the thermal lens as the Fresnel number decreases.

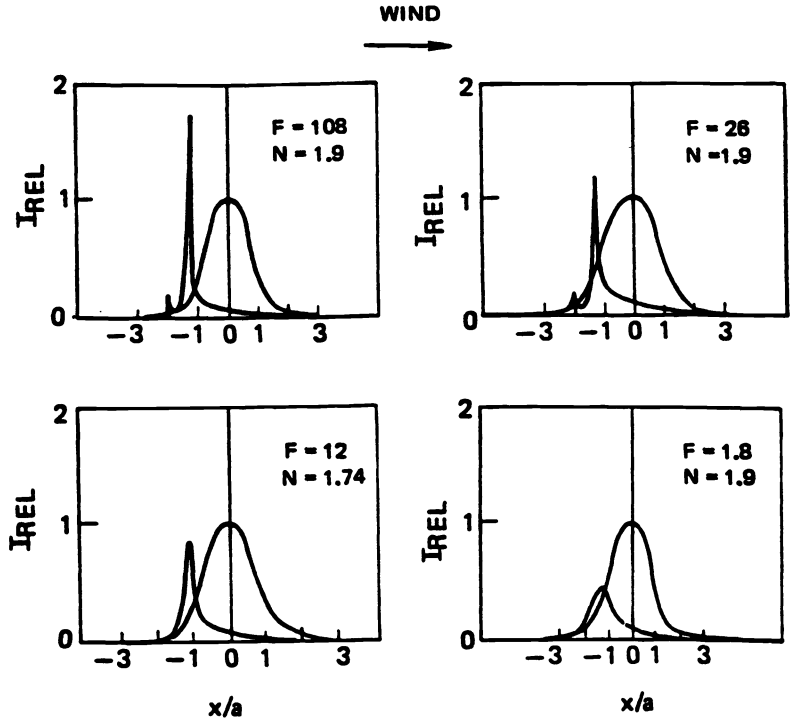

Figure 5. Measured Fresnel number dependence of bloomed intensity for $N_C \approx 2$.[33]

4.2 Focused Beams - Inhomogeneous Paths

The effects of convection dominated thermal blooming for focused beams, including the effects of beam slewing and finite attenuation, have been studied extensively using laboratory simulation experiments, ray-optics perturbation theories and detailed wave-optics propagation codes.[1-6] Although the wave-optics codes can provide a comprehensive and accurate treatment of this problem as well as a variety of other more complicated blooming problems, e.g., for stagnation zones, transonic slewing, optical turbulence, and phase compensation, simple analytical scaling relations are more convenient and often adequate for providing useful approximations for the blooming effects on the peak irradiance. Such a scaling parameter has been found by using the integral expression in (12) to obtain a generalized beam distortion parameter that accounts for beam focusing and non-uniform winds and beam heating effects.[3] The generalized beam distortion parameters[3] is

$$N = N_C \, f(N_E) q(N_F) s(N_\omega) \tag{16}$$

where $N_C = N_D/2\pi N_F$ is the distortion parameter defined earlier (Eq. 14) for a collimated beam and the functions f, q and s, which , respectively, represent correction factors for the effects of finite attenuation (i.e., when the extinction number N_E is not small), the focusing or divergence of the laser beam and the nonuniform velocity profile with beam slewing, are given by

$$f(N_E) = (2/N_E^2)[N_E - 1 + \exp(-N_E)] \quad (17)$$

$$q(N_F) = \left[2N_F^2/(N_F-1)\right]\left[1 - \ell n\ N_F/(N_F-1)\right] \quad (18)$$

$$s(N_\omega) = (2/N_\omega^2)\left[(N_\omega+1)\ell n(N_\omega+1) - N_\omega\right] \quad (19)$$

The Fresnel number N_F, defined earlier, gives the degree of focusing a_o/a for a focused diffraction limited beam where a_o and a are the beam sizes at the source and focal range z, respectively. The slewing number $N_\omega = \omega z/v_o$, where ω is the slew rate (assumed to be in the direction opposite to the wind), is the ratio of the beam slewing speed at z to the uniform wind speed v_o. The general beam distortion parameter N thus depends on the four dimensionless parameters N_C, N_F, N_E and N_ω. Bradley and Herrmann[27] have shown that these four parameters completely characterize the thermal blooming problem for this case. It is interesting to note that when the beam is strongly focused (i.e., $N_F >> 1$) without slewing ($N_\omega = 0$) and, with $N_E << 1$, the beam distortion number reduces to $N \approx N_D/\pi$. This means that the peak intensity of the focused beam, relative to the unbloomed value, I_{REL} or equivalently, the Strehl ratio, in the small perturbation limit, depends on the "phase" distortion number according to $1-(1/2\sqrt{\pi})N_D$. This is in contrast to the collimated beam case where I_{REL} decreases as $1 - (1/4\sqrt{\pi})N_D/N_F$.

The general beam distortion parameter N has proven useful as a simple empirical correlation or scaling parameter for approximating thermal blooming effects in terms of the four parameters N_D, N_F, N_E and N_ω. For example, Figure 6 shows that the experimental and wave-optics code results are reasonably well

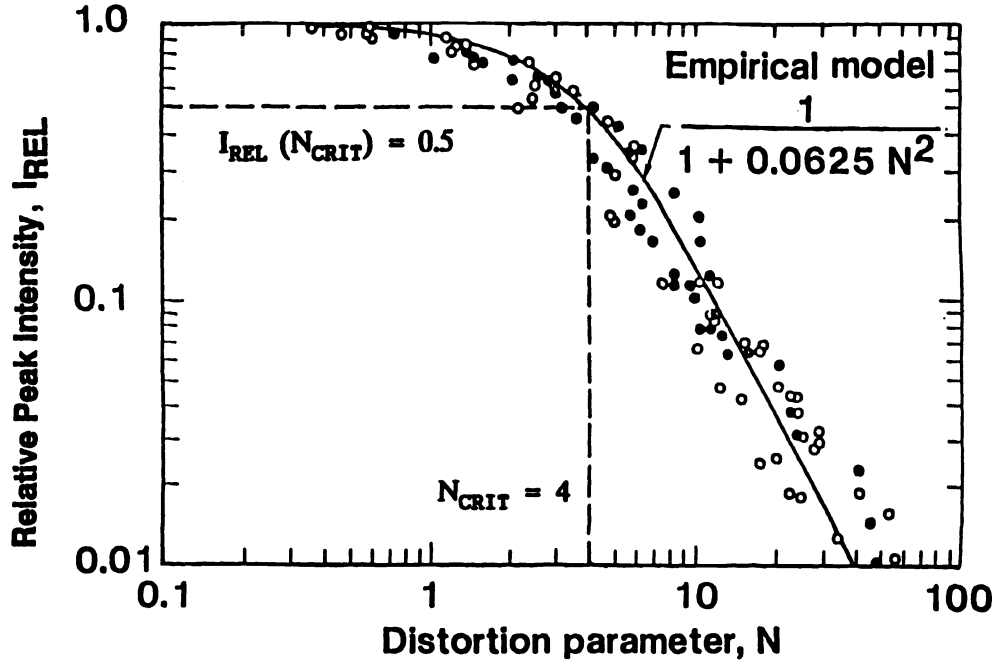

Figure 6. Blooming I_{REL} dependence on the parameter N for experimental and wave-optics code results.[3]

correlated by the beam distortion parameter N with the simple empirical expression[3]

$$I_{REL}(N) = [1 + 0.0625\ N^2]^{-1} \qquad (20)$$

The experimental results include data from several different measurements for focused beams with $N_F = 7$, $N_E = 0.4$ and without slewing ($N_\omega = 0$). The code results were obtained for Gaussian focused beams for the following wide range of conditions: $N_F = 3, 6, 10, 18, 28$ and 66; $N_E = 0.1, 0.4$ and 0.6; and $N_\omega = 0, 3.8$ and 8.

Figure 7 shows a comparison of results from a laboratory experiment and a wave-optics code calculation for the bloomed irradiance pattern of a focused Gaussian beam for very different conditions but with comparable beam distortion numbers N of 13 and 16, respectively.[3] The measured and calculated beam patterns are very similar in appearance and have comparable values of I_{REL} of 0.05 and 0.07 and for the normalized shift in peak intensity of 6 and 4.4, respectively.

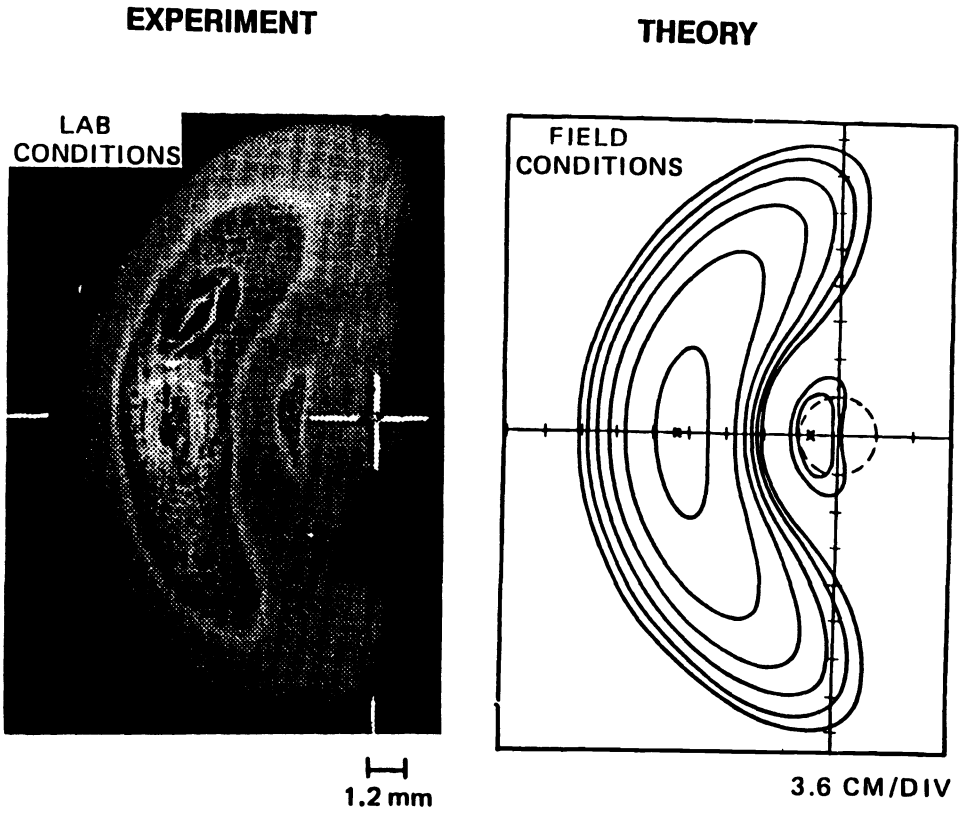

Figure 7. Thermal blooming patterns from laboratory experiment (N = 13) and code calculation (N = 16).[3]

The conditions for the laboratory blooming experiment and for the code calculation of a field-scale propagation scenario are compared in Table 2.[3]

An important characteristic of the thermal blooming process is its effect in limiting the peak irradiance that can be propagated to a maximum or critical value I_c, independent of the available power at the transmitter. The power at which the critical intensity is achieved is called the critical power, P_c; and since $P \sim N$, P_C corresponds to the value of $N = N_{CRIT}$ where the slope of the I_{REL} (N) versus N curve (see Figure 6) has a slope of -1. This follows since the peak intensity, given by the product of the unbloomed peak I_{PO} and I_{REL}, no

Table 2. Conditions for Simulation Experiment and Wave Optics Code Results in Fig. 7.[3]

	Simulation experiment	Wave optics code results
	Lab conditions	Field conditions
Medium	CO_2 at 10 atm	Atmospheric air
Absorption coefficient,cm^{-1}	4×10^{-3}	7×10^{-7}
Wind velocity, cm/sec	1	200
Wavelength, μm	10.6	10.6
Power, W	9	10^5
Beam diameter, cm	0.9	28.3
Range, m	1	2×10^3
Beam distortion, N	13	16
Extinction, N_E	0.41	0.134
Fresnel, N_F	2.6	2.8
Relative irradiance, I_{REL}	0.05	0.07
Peak deflection, $\Delta x/a$	6	4.4

longer increases with I_{PO}, which increases linearly with the power, when I_{REL} begins to decrease inversely with power, or, equivalently N. Figure 8 shows the peak intensity versus power curve for thermal blooming, based on the empirical model (Eq. 20) for $I_{REL}(N)$ shown in Figure 6, where $N_{CRIT} = 4$ and $I_{REL}(N_{CRIT}) = 0.5$. The critical or optimum power effect with blooming is clearly shown in Figure 8 where, although the peak intensity initially increases linearly with power ($P << P_c$), the maximum is reached when $P = P_c$ and any further increase in power causes the intensity to decrease.

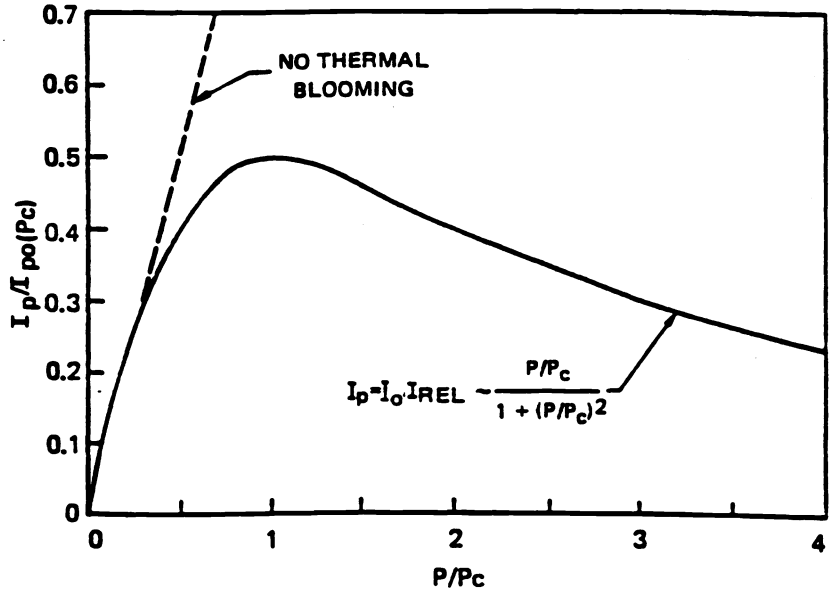

Figure 8. Peak irradiance versus power with thermal blooming.[3]

A similar empirical scaling law I_{REL} (N) has been found to apply for a uniform irradiance beam and is given with the constant factor and exponent in (20) replaced with 0.09 and 1.22, respectively.[4] In this case N_{CRIT} = 25 and I_{REL} (N_{CRIT}) = 0.18, indicating the significantly reduced blooming effects which occur for the uniform versus the Gaussian beam shape.

An example of a direct comparison of a detailed 4-D wave optics blooming code calculation made with a laboratory simulation experiment is shown in Figure 9.[34]

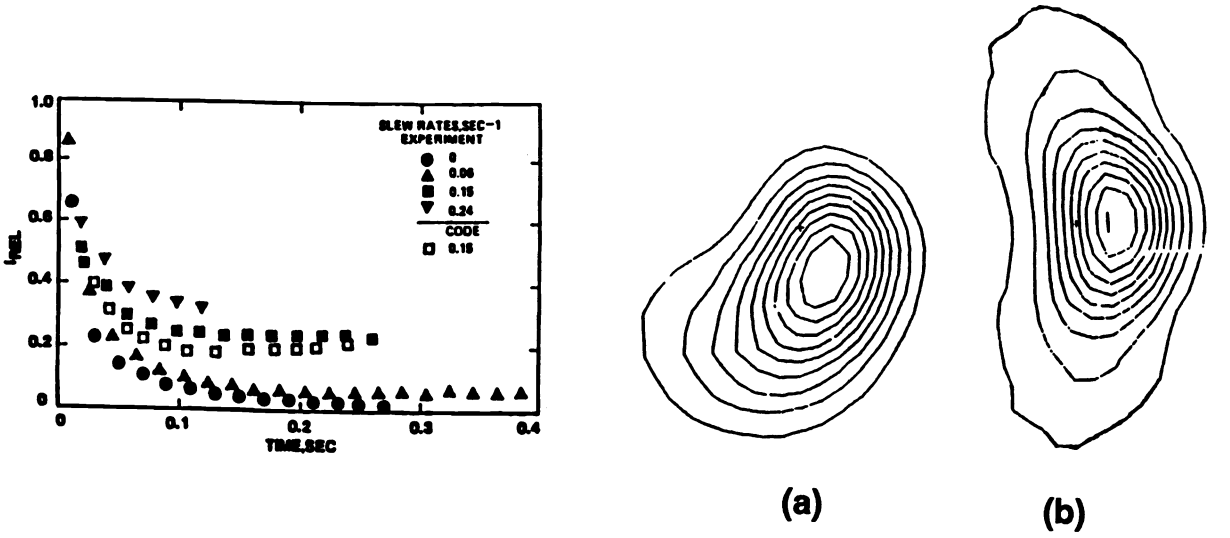

Figure 9. Relative intensity vs. time results for 4-D code and experiment for stagnation zone blooming. Calculated blooming patterns are at 0.1 sec with (a) and without (b) natural convection.[34]

The blooming problem studied here is complicated considerably by the combined effects of a focussed beam with slewing horizontally, a stagnation region (i.e., with zero flow or beam motion) mid-way along the propagation path and with natural convection vertical flow efffects also included. The code results are in good agreement with the experiment for the 0.15 rad/s case compared in Figure 9. The calculated bloomed beam patterns shown in Figure 9 are for the time of 0.1 sec with (a) significant natural convection effects evident, which is the case compared with the experiment, and (b) with natural convection neglected. These results as well as a number of other detailed comparisons of the propagation codes with laboratory blooming experiments have shown the code calculations of whole beam thermal blooming effects to be in good agreement with the experiments.[4]

4.3 Up-link Thermal Blooming

In this section we consider thermal blooming for an up-link or ground-to-space propagation path. A simple ray-optics model is shown to provide a good approximation for the peak far-field Strehl ratio for uncorrected up-link blooming. The ray-optics model for the phase conjugate corrected up-link blooming Strehl ratio is then used to obtain the whole-beam instability limit for up-link phase compensation.

Figure 10 shows the geometry for the up-link blooming problem. We assume a uniform irradiance beam with power P and diameter D propagating from the laser altitude H_L to the range R in space where it is focused. The laser beam can be considered to be well collimated, with the same uniform irradiance as at the source, within the sensible atmosphere (i.e., $H_L \leq z \leq H_A$) since (1) the focal range R is much larger than the range H_A - H_L through the atmosphere; and, (2) both diffraction and blooming effects on the beam irradiance

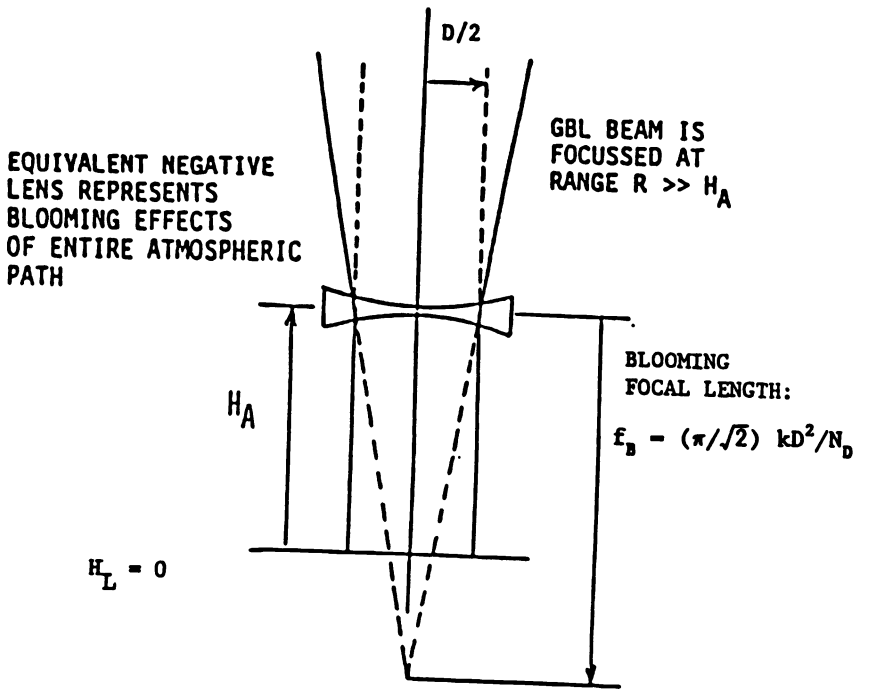

Figure 10. Geometry for up-link blooming

within the atmosphere are small for the large Fresnel numbers (i.e., short wavelengths, large aperture sizes and short atmospheric heating paths) which are typically of interest. The thermal blooming effect on the far-field Strehl ratio is thus determined by the blooming phase for the uniform collimated beam at the top of the atmosphere. From Section 4.1 the blooming phase can be approximated by that for a cylindrical negative lens with focal length

$$f_B = (\pi/\sqrt{2})\ kD^2/N_D \tag{21}$$

Here, $N_D = N_D(H_A)$ is the total of the cumulative distortion number $N_D(H)$ for the entire up-link path. $N_D(H)$ is a generalization by Herrmann of the original Bradley-Herrmann N_D (Eq. 9),[27] which describes the distribution of the thermal blooming, as a function of altitude, for up-link propagation. It is defined by

$$N_D(H,\theta_z) = \frac{C_A kP \sec\theta_z}{D} \int_{H_L}^{H} \frac{\alpha_T(h)\ T_0\ t(h)}{V_E(h)\ T(h)}\, dh \tag{22}$$

where

$$C_A = 5.66(-n_T)/\rho_0 C_p = 4.72 \times 10^{-9}\ m^3/J \tag{23}$$

is the atmospheric refractivity constant for air at temperature T_o = 273 K. The other parameters in Eq. 22 not previously defined are

θ_z = path zenith angle

$\alpha_T(h) = k_m(h) + k_a(h)$ (total absorption coefficient)

$k_m(h)$ = molecular absorption coefficient

$k_a(h)$ = aerosol absorption coefficient

$\sigma_T(h) = \sigma_m(h) + \sigma_a(h)$ (total scattering coefficient)

$\sigma_m(h)$ = molecular scattering coefficient

$\sigma_a(h)$ = aerosol scattering coefficient

$V_E(h)$ = effective cross-wind speed including slewing

$T(h)$ = air temperature

$t(h)$ = cumulative transmittance

$$= \exp\left\{ - \sec \theta_z \int_{H_L}^{h} [\alpha_T(h') + \sigma_T(h')]\, dh' \right\} \qquad (24)$$

The peak far-field Strehl ratio at the target range R due to the uncorrected blooming is then found by forming the ratio of the area of the diffraction limited spot with radius $a_D \sim R\lambda/D$ to the root-sum-squared spot area due to diffraction and blooming combined where the blooming radius, from Figure 10, is $a_B \sim RD/2f_B$. The Strehl ratio for uncorrected blooming is then

$$SR_{BU} = [1 + N_D^2/8\pi^4]^{-1/2} \qquad (25)$$

and depends only on the total phase distortion parameter N_D.

Figure 11 shows the uncorrected blooming Strehl ratio dependence on the distortion number N_D, which is proportional to the laser beam power, for a particular case of up-link propagation at zenith for a 1m diameter excimer laser beam at $\lambda = 0.35\ \mu m$. The distortion number N_D in this case is ~70 at the critical power where the Strehl has dropped to about 0.35. Also shown for comparison with the ray optics model results in Figure 11 are wave optics code results for the same case. The agreement between the ray-optics model and the wave optics code results is very good except at the larger distortion values where the effects of the fourth and higher order terms in the blooming phase, which are not included in the ray-optics model, become important.

For phase compensated up-link blooming we consider the situation shown in Figure 12 where the blooming is limited to a discrete thin layer of thickness ΔZ_B, centered at the altitude Z_B above the transmitter. Following the same procedure as before, the effect of the blooming layer of thickness ΔZ_B is represented by the equivalent negative cylindrical lens of focal length $f_B(Z_B)$. Here, $f_B(Z_B)$ is given by Eq. 21 but with $N_D(H_A)$ replaced with the value of the cumulative distortion parameter $N_D(\Delta Z_B;Z_B)$ appropriate for the thickness and position for the particular blooming layer in question.

As shown in Figure 12, the effect of the negative cylindrical lens associated with the blooming layer at height Z_B is to spread the beacon return wave intercepted by the negative lens of diameter D such that it overfills the transmitter aperture at ground level. Perfect phase conjugate compensation consists simply of focusing the up-link beam to the range $Z_B + f_B$. The focusing correction results in the slightly smaller beam diameter D_C at the altitude Z_B of the blooming layer, as shown on Figure 12. Above the blooming layer the up-link beam emerges perfectly collimated, however, since the original negative cylindrical thermal lens due to the blooming layer exactly cancels the focusing correction applied to the up-link beam.

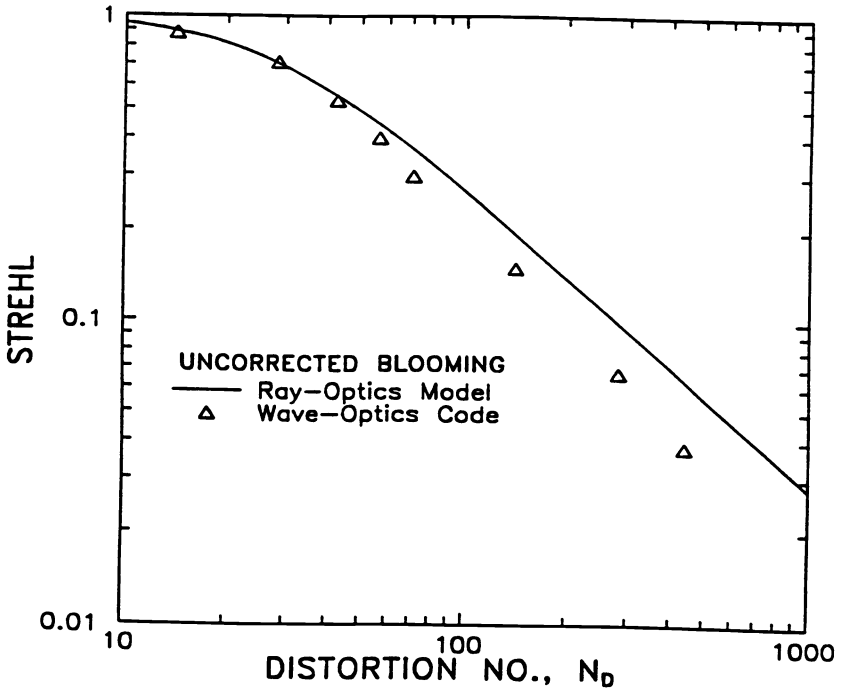

Figure 11. Comparison of ray-optics model and wave-optics code results for up-link blooming.

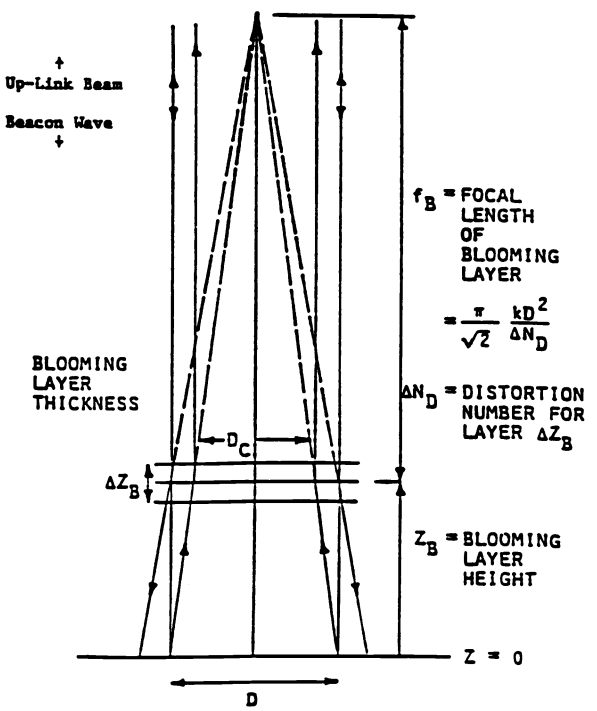

Figure 12. Geometry for phase compensated up-link blooming.

From Figure 12, the reduced beam diameter D_C at the height of the blooming slab Z_B, is given by

$$D_C/D = f_B/(f_B + Z_B) \tag{26}$$

The reduced beam size D_C at the blooming layer results in two things. First, the irradiance is increased which increases the strength of the blooming layer at Z_B. From Eqs. (21) and (22) the focal length of the blooming layer, as a result of the phase correction, is decreased to the following value

$$f_{BC} = (D_C/D)^3 f_B \tag{27}$$

Now, according to Eq. (26), correction of the new blooming phase associated with f_{BC}, results in a further reduction in the beam diameter D_C.

The phase conjugate correction process proceeds in an iterative fashion until a stable, self-consistent solution is obtained for Eqs. (26) and (27), with f_B replaced with f_{BC} in Eq. (26). Combining Eqs. (26) and (27) gives the following cubic equation for $x = D_C/D$

$$x^3 - x^2 + (Z_B/f_B) = 0 \tag{28}$$

which must be satisfied when the phase conjugate correction process has converged.

The second effect of the reduced beam size D_C, which results from the phase conjugate correction of blooming for the layer at altitude Z_B, is the reduction in the far-field Strehl ratio and is given by

$$SR_{BC} = D_C/D = [1 + (D/D_C)^3 Z_B/f_B]^{-1} \tag{29}$$

This reduction in the far-field Strehl ratio occurs because the beam spreading angle after phase correction increases from λ/D (without correction) to the value λ/D_C. (Note that this occurs only in the plane transverse to the wind where the blooming spreads the beam.)

The solution to Eqs. (28) or (29), which are equivalent, is given by

$$SR_{BC} = \frac{1}{3} + \frac{2}{3}\cos[\frac{1}{3}\cos^{-1}(1 - 13.5 Z_B/f_B)] \tag{30}$$

Equation (30) provides a physically meaningful (i.e., real) solution for the Strehl only if $Z_B/f_B \leq 4/27$. This means that stable phase conjugate correction of the blooming layer of strength $\sim 1/f_B$ at the range Z_B, is limited to the conditions where

$$0 \leq Z_B/f_B \leq (4/27) \approx 0.148 \tag{31}$$

Thus, when Z_B/f_B is small, corresponding either with weak blooming (i.e., large f_B) or, equivalently, with stronger blooming which occurs very close to the transmitter aperture (i.e., small Z_B) phase correction is very effective with the Strehl ratio SR_{BC} approaching unity. As Z_B/f_B increases, phase correction becomes less effective until, at $Z_B/f_B = 4/27$, where the minimum stable corrected Strehl $SR_{BC} = 2/3$, occurs. For $Z_B/f_B > 4/27$, the phase conjugate correction does not converge to a stable improvement over the uncorrected value but, rather drives the Strehl ratio SR_{BC} to zero. This clearly shows the limit imposed on the phase compensation of whole-beam thermal blooming due to the finite range Z_B of the blooming region from the aperture, i.e., $Z_B \leq 0.148\ f_B$ for stable phase correction. Similar results showing that stable phase conjugate correction of thermal blooming can only be obtained for a limited range of the strength of the blooming were first reported by Herrman[35] for the case of laser beams focused within the blooming region.

The phase correction model for the single thin blooming layer can be extended to the more interesting case of a distributed blooming region by using the value of f_B given in Eq. (21) for the entire atmospheric path and by using, for the effective blooming layer range Z_B, the appropiately normalized first moment, with respect to range, of the atmospheric heating distribution function

$$f_H(h) = \alpha_t(h)T_o t(h)/V_E(h)T(h) \tag{32}$$

Recognizing that f_H is the integrand in Eq. (22) for the distortion parameter N_D, the effective blooming range Z_B is given by

$$Z_B = \frac{C_A k P \sec^2\theta_z}{N_D D} \int_{H_L}^{H_A} (h-H_L)\, f_H(h)\, dh \tag{33}$$

The corrected blooming Strehl ratio given by Eq. (30) is shown in Figure 13 for the same laser beam and atmospheric conditions used earlier for the excimer laser case in Figure 11. For this case where the effective blooming range Z_B is 12.7 km and the whole-beam Fresnel number N_F is 177 we have that $Z_B/f_B = (1/\pi 2^{5/2})N_D/N_F \approx 3.18 \times 10^{-4}\, N_D$.

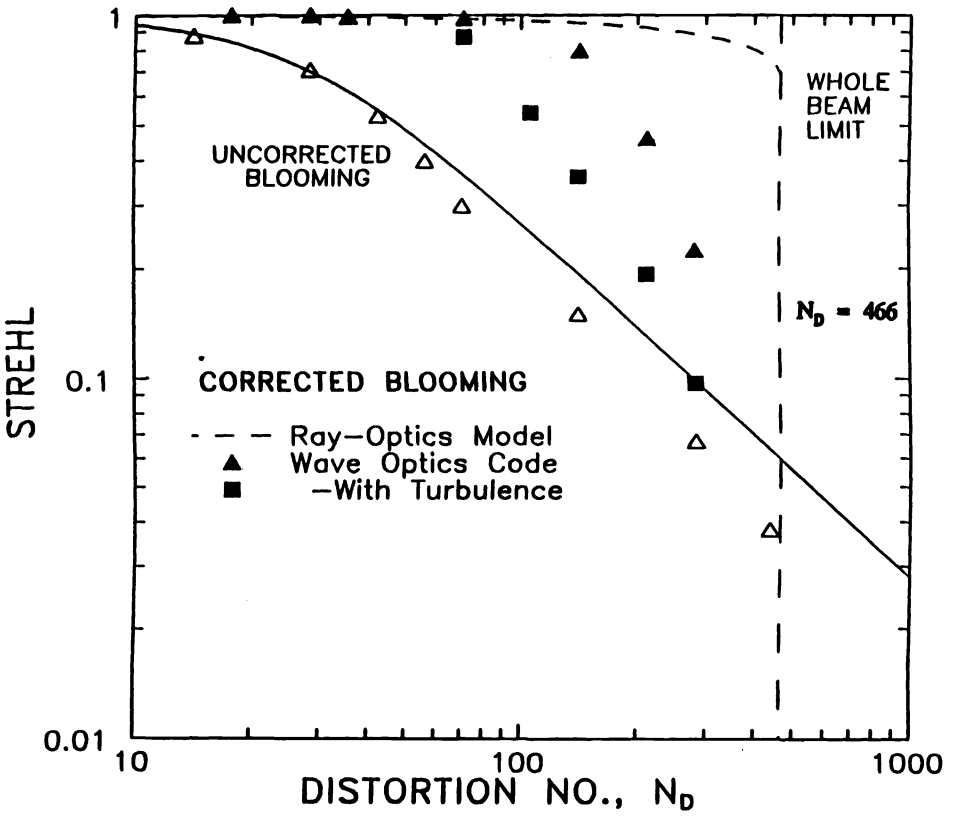

Figure 13. Comparison of ray-optics model and wave-optics code results for phase compensated up-link blooming.

The vertical dashed line shows the whole-beam limit for stable blooming phase correction, which for this case occurs at N_D = 466. At larger blooming distortion values the phase conjugate correction leads to unstable conditions with reduced Strehl due to the increased atmospheric heating and beam distortion at high altitudes caused by the run-away focusing correction.

The condition $Z_B/f_B \leq 0.148$ for the whole-beam limit for phase corrected blooming can also be expressed as $N_D/N_F \leq 2.6$ or $N_C \leq 0.42$, where we have used Eq. (21) for f_B for the uniform beam and the Fresnel number is given by $N_F = kD^2/8Z_B$. For the infinite Gaussian beam shape the whole-beam correction limits are $N_D/N_F \leq 0.53$ and $N_C \leq 0.086$ which are about a factor of five smaller than for the uniform beam. From these small values of N_C it is clear that stable phase correction can be achieved only if the whole beam blooming distortion without correction is kept very small within the effective range Z_B of the up-link blooming layer. Since $N_D \sim P/D$ and $N_F \sim D^2$ the whole-beam limit for the up-link correctable power is seen to scale as D^3.

The wave-optics code results for phase corrected blooming alone shown in Figure 13 do not achieve the high Strehl ratios predicted by the ray-optics model (Eq. 30) for distortion conditions well below the whole-beam limit for phase correction. With turbulence (with the coherence length r_o = 3.3 cm) and blooming together the code results for the corrected Strehl fall off even more rapidly with distortion number. The calculated Strehls are being limited by the effects of small-scale blooming instabilities which, for the uniform wind direction case, appear as striations parallel with the wind in the beam irradiance and phase. Figure 14 shows an example, obtained with SAIC's APAC code, of the small-scale blooming distortions in the beacon wave intensity and phase at the ground with phase compensated turbulence and blooming for a Gaussian beam with the conditions λ = 1.06 μm, N_D = 60, N_F = 237, turbulence coherence length r_o = 7.6 cm and a deformable mirror actuator spacing d_A of 5 cm. Here $N_D/N_F \sim 0.25$, which is only about one-half the whole beam correction limit. The Strehl of the high energy up-link beam has decreased to about 0.6 for this case compared with the values of about 0.9 obtained at low power without blooming or about 0.96 with just blooming alone. Recent progress in the analysis and modeling of the small-scale blooming effects on up-link phase compensation is reported in a number of subsequent papers in this proceedings.

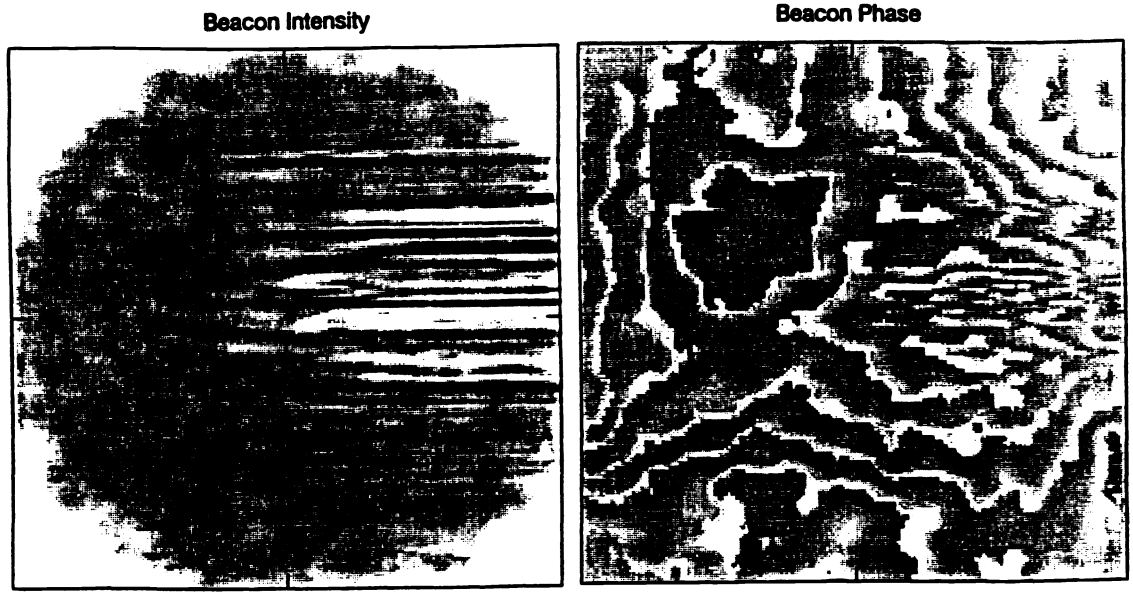

Figure 14. Beacon intensity and phase at the ground with phase compensated turbulence and blooming for the conditions: λ = 1.06 μm, N_D = 60, N_F = 237, r_o = 7.6 cm, and actuator spacing d_A = 5 cm.

5. CONCLUSIONS

An overview has been presented of the work performed on thermal blooming over the past twenty-five years since the first observations were reported. A brief historical overview and a review of the governing equations and basic characteristics of the different types of blooming problems for CW, SP and RP laser beams were given. The remaining discussion concentrated on the problem of convection dominated thermal blooming, which is the most important blooming problem for CW or RP HEL beam propagation in the atmosphere. The important results and scaling parameters for describing steady-state convection dominated whole-beam thermal blooming effects were reviewed for: (1) a collimated beam in a homogeneous atmosphere; (2) focused beam propagation including the combined effects of wind and beam slewing and finite attenuation ; and, (3) ground-to-space propagation both with and without phase compensation. In addition to causing severe beam spreading, bending and distortion the most serious problem which occurs with all types of thermal blooming, is the limit it imposes on the maximum useful power that can be propagated through the atmosphere and concentrated within a small spot, of the order of the diffraction limited beam size, at the target. Dimensionless parameters and simple scaling laws were presented which can be used to determine the maximum or critical power limits due to whole-beam thermal blooming. A simple ray-optics model for phase conjugate correction of up-link thermal blooming was presented and used to show that stable correction is limited by whole-beam blooming effects to conditions where the beam distortion within the blooming region is small, i.e., the beam distortion parameter $N_C = (1/2\pi)N_D/N_F$ must be less than ~0.09 and 0.4, respectively, for Gaussian and uniform beams. This requirement implies a corrected critical power scaling with D^3. Propagation code results for phase compensated up-link blooming alone, and also combined with turbulence, were shown with small-scale blooming instabilities limiting the effectiveness of phase correction to distortion numbers well below the whole-beam critical distortion limit. Current studies of thermal blooming, as shown in a number of the subsequent papers, are concentrating on developing a comprehensive understanding of and modeling and analysis capability for the small-scale blooming instability effects and limits on phase compensated HEL beam propagation in atmosphere.

6. ACKNOWLEDGEMENTS

This work was sponsored in part by SDIO and performed on sub-contract No. SC-88W-34-003 with W. J. Schafer Associates, Inc., under prime contract No. SDIO84-88-C-0057 with the Strategic Defense Initiative Organization, The Pentagon, Washington, D. C. The author wishes to express his appreciation to his colleagues S. A. Mani, J. E. Long, R. E. Hodder, L. S. Hills and R. C. Wade for many helpful discussions and for their efforts in support of the up-link propagation modeling and analysis work. He is also grateful to P. B. Ulrich of W.J. Schafer Associates, Inc. for his encouragement and suggestions for the preparation of this review.

7. REFERENCES

1. C. B. Hogge, "Propagation of High Energy Laser Beams in the Atmosphere," in Physics of Quantum Electronics, Vol. 1, High Energy Lasers and Their Applications, Edited by S. Jacobs, M. Sargent III and M. O. Scully, pp. 177-246, Addison Wesley, Reading, MA, 1974.

2. J. N. Hayes, "Propagation of High Energy Laser Beams through the Atmosphere: An Overview," AGARD Conf. Proc. No. 183. Optical Propagation in the Atmosphere, Section 27, May 1976.

3. F. G. Gebhardt, "High Power Laser Propagation," Appl. Opt. Vol. 15, No. 6, pp. 1479-1493, June 1976.

4. D. C. Smith, "High-Power Laser Propagation: Thermal Blooming," Proc. IEEE Vol. 65, No. 12, pp. 1679-1714, Dec. 1977.

5. J. L. Walsh and P. B. Ulrich, "Thermal Blooming in the Atmosphere," in Laser Beam Propagation in the Atmosphere, J. W. Strohbehn, ed., Springer - Verlag, New York, 1978.

6. F. G. Gebhardt, "Overview of Atmospheric Effects on Propagation of High Energy Laser Radiation," SPIE Proceedings Vol. 195, Atmospheric Effects on Radiative Transfer, pp. 162-170, 1979.

7. T. J. Karr, "Thermal Blooming Compensation Instabilities," J. Opt. Soc. Am. A Vol. 6, No. 7, pp. 1038-1048, July 1989.

8. K. A. Breuckner and S. Jorna, "Linearized Theory of Laser Induced Instabilities in Liquids and Gases," Phys. Rev. Vol. 164, pp. 182-193, 1967.

9. N. M. Kroll and P. L. Kelley, "Temporal and Spatial Gain in Stimulated Light Scattering," Phys. Rev. A. Vol. 4, pp. 763-776, 1971.

10. J. P. Gordon, R. C. C. Leite, R. S. Moore, S. P. S. Porto, and J. R. Whinnery, Bull. Am. Phys. Soc. Ser. II, Vol. 9, p. 501, 1964.

11. J. P. Gordon, R. C. C. Leite, R. S. Moore, S. P. S. Porto, and J. R. Whinnery, "Long Transient Effects in Lasers with Inserted Liquid Samples," J. Appl. Phys. Vol. 36, pp. 3-7, 1965.

12. K. E. Rieckhoff, "Self-induced Divergence of CW Laser Beams in Liquids - A New Nonlinear Effect in the Propagation of Light," Appl. Phys. Letters Vol. 9, p. 87, 1966.

13. W. R. Callen, B. G. Huth, and R. H. Pantell, "Optical Patterns of Thermally Self-defocused Light," Appl. Physics Letters Vol. 11, p. 103, 1967.

14. J. R. Whinnery, D. T. Miller, and F. Dabby, "Thermal Convection and Spherical Aberration Distortion of Laser Beams in Low-Loss Liquids," IEEE J. Quantum Electron Vol. QE-3, p. 382, 1967.

15. H. Inaba and H. Ito, "Observation of Power-Dependent Distortion of an IR Beam at 10.6 μ from a CO_2 Laser," IEEE J. Quantum Electron. Vol. QE-4, p. 45, 1968.

16. R. L. Carman and P. L. Kelley, "Time Dependence in the Thermal Blooming of Laser Beams," Appl. Phys. Letters Vol. 12, p. 241, 1968.

17. R. C. C. Leite, R. S. Moore, and J. R. Whinnery, "Low Absorption Measurements by Means of the Thermal Lens Effect Using an He-Ne Laser," Appl. Phys. Letters Vol. 5, p. 141, 1964.

18. D. Solimini, "Loss Measurements of Organic Materials at 6328 Å," J. Appl. Phys. Vol. 37, p. 3314, 1966.

19. D. Solimini, "Accuracy and Sensitivity of the Thermal Lens Method for Measuring Absorption," Appl. Opt. Vol. 5, p. 1931, 1966.

20. R. C. C. Leite, S. P. S. Porto, and T. C. Damen, "The Thermal Lens Effect as a Power-Limiting Device," Appl. Phys. Letters Vol. 10, p. 100, 1967.

21. S. A. Akhmanov, D. P. Krindach, A. V. Migulin, A. P. Sukhorukov and R. V. Khokhlov, "Thermal Self-Actions of Laser Beams," IEEE J. Quantum Electron. Vol. QE-4, No. 10, pp. 568-575, Oct. 1968.

22. F. G. Gebhardt and D. C. Smith, "Effects of Wind on Thermal Defocusing of CO_2 Laser Radiation," Appl. Phys. Letters Vol. 14, No. 2, pp. 52-54, Jan. 1969.

23. D. C. Smith, "Thermal Defocusing of CO_2 Laser Radiation in Gases," IEEE J. Quantum Electron. Vol. QE-5, pp. 600-607, Dec. 1969.

24. A. J. Glass, "Thermal Blooming in Gases," Opto-Electronics Vol. 1, pp. 174-178, 1969.

25. D. M. Cordray and P. B. Ulrich, "Computer Techniques for Solution of the High-Energy Laser Propagation Problem," SPIE Proceedings Vol. 195, Atmospheric Effects on Radiative Transfer, pp. 182-191, 1979.

26. F. G. Gebhardt, D. C. Smith, R. G. Buser, and R. S. Rohde, "Turbulence Effects on Thermal Blooming," Appl. Opt., Vol. 12, no. 8, pp. 1794-1805, Aug. 1973.

27. L. C. Bradley and J. Herrmann, "Phase Compensation for Thermal Blooming," Appl. Opt., Vol. 13, no. 2, pp. 331-334, Feb. 1974.

28. E. L. O'Neill, Introduction to Statistical Optics, Chapter 4, Addison-Wesley, Reading MA, 1964.

29. The pincushion distortion is readily identified in experimental measurements of blooming effects on target image quality (e.g., see F. G. Gebhardt, "Self-Induced Thermal Distortion Effects on Target Image Quality," Appl. Opt. Vol. 11, No. 6, pp. 1419-1423, June 1972). An example of pincushion distortion is also shown in Figure 4-7 of Reference 28.

30. F. G. Gebhardt and D. C. Smith, "Self-Induced Thermal Distortion in the Near Field for a Laser Beam in a Moving Medium," IEEE J. Quant. Electron. QE-7, No. 2, pp. 63-73, Feb. 1971.

31. R. J. Hull, P. L. Kelley, and R. L. Carman, "Self-induced Thermal Lens Effect in CCl_4 in the Presence of Beam Motion," Appl. Phys. Letts., Vol. 17, pp. 539-541, Dec. 15, 1970.

32. D. C. Smith and F. G. Gebhardt, "Saturation of the Self-induced Thermal Distortion of Laser Radiation in a Wind," Appl. Phys. Letts., Vol. 16, No. 7, pp. 275-278, Apr. 1, 1970.

33. F. G. Gebhardt and D. C. Smith, "Effects of Diffraction on the Self-induced Thermal Distortion of a Laser Beam in a Crosswind," Appl. Opt., Vol. 11, No. 2, pp. 244-248, Feb. 1972.

34. P. J. Berger, P. B. Ulrich, J. T. Ulrich, and F. G. Gebhardt, "Transient Blooming of a Slewed Laser Beam Containing a Region of Stagnant Absorber," Appl. Opt., Vol. 16, No. 2, pp. 345-354, Feb. 1977.

35. J. Herrmann, "Properties of Phase Conjugate Adaptive Optical Systems," J. Opt. Soc. Am., Vol. 67, No. 3, pp. 290-295, March 1977.